Crystal structure of cephalexin monohydrate, $C_{16}H_{17}N_3O_4S(H_2O)$

James A. Kaduk,[1,2,a] Amy M. Gindhart,[3] and Thomas N. Blanton[3]
[1]*Illinois Institute of Technology, 3101 S. Dearborn St., Chicago, IL 60616, USA*
[2]*North Central College, 131 S. Loomis St., Naperville, IL 60540, USA*
[3]*ICDD, 12 Campus Blvd., Newtown Square, PA 19073-3273, USA*

(Received 11 August 2020; accepted 30 September 2020)

The crystal structure of cephalexin monohydrate has been solved and refined using synchrotron X-ray powder diffraction data and optimized using density functional techniques. Cephalexin monohydrate crystallizes in space group *C*2 (#5) with $a = 27.32290(17)$, $b = 11.92850(4)$, $c = 16.75355(8)$ Å, $\beta = 108.8661(4)°$, $V = 5166.99(3)$ Å^3, and $Z = 12$. Although the general arrangement of molecules is similar to that in cephalexin dihydrate, the structural differences result in very different powder patterns. The crystal structure is characterized by alternating layers of hydrogen bonds and van der Waals contacts parallel to the *bc*-plane. The water molecules occur in clusters. Five of the six protons in the water molecules act as donors in O–H···O hydrogen bonds. The sixth hydrogen atom acts as a donor to two different phenyl ring carbon atoms to form bifurcated O–H···C hydrogen bonds. Each cephalexin molecule is a zwitterion, containing ammonium and carboxylate groups. The ammonium ions form N–H···O hydrogen bonds to carboxylate groups and water molecules, as well as to carbonyl groups. The powder pattern is included in the Powder Diffraction File™ as entry 00-065-1417. © *2020 International Centre for Diffraction Data*. [doi:10.1017/S0885715620000627]

Key words: cephalexin, powder diffraction, Rietveld refinement, density functional theory

I. INTRODUCTION

Cephalexin monohydrate (trade names Aristosporin, Keflex) is a first-generation β-lactam cephalosporin antibiotic. It kills Gram-positive and some Gram-negative bacteria by disrupting the growth of the bacterial cell wall. Cephalexin monohydrate is used to treat respiratory, urinary tract, bone, and skin bacterial infections by preventing bacteria from forming cell walls that surround each cell. It works similarly to other cephalosporins but can be taken orally. The IUPAC name (CAS Registry number 23325-78-2) is (6*R*,7*R*)-7-[[(2*R*)-2-amino-2-phenylacetyl]amino]-3-methyl-8-oxo-5-thia-1-azabicyclo[4.2.0]oct-2-ene-2-carboxylic acid hydrate. A two-dimensional molecular diagram (without H_2O) is shown in Figure 1.

Indexed powder patterns of cephalexin monohydrate are contained in the Powder Diffraction File (Gates-Rector and Blanton, 2019), entries 00-040-1653 (Sonneveld, 1989; space group *Im*) and 00-045-1537 (Jenkins and Stevenson, 1990; space group $P2_1/m$). A star-quality pattern generated from the synchrotron data set of this paper is present as entry 00-065-1417. A star-quality pattern of cephalexin dihydrate is contained in PDF entry 00-040-1652 (Sonneveld, 1989; space group *Im*), and a primary pattern calculated from a 150 K crystal structure is contained in the PDF-4/Organics database as entry 02-084-1771 (Kennedy *et al.*, 2003). Powder data for cephalexin monohydrate are reported in US Patent 3,862,186 (Silvestri, 1975; Bristol-Myers). Powder patterns for cephalexin monohydrate, dihydrate, and several solvates are reported in Pfeiffer *et al.* (1970). Several of these patterns, as well as patterns for cephalexin hydrochloride derivatives, are contained in the PDF.

This work was carried out as part of a project (Kaduk *et al.*, 2014) to determine the crystal structures of large-volume commercial pharmaceuticals and include high-quality powder diffraction data for these pharmaceuticals in the Powder Diffraction File.

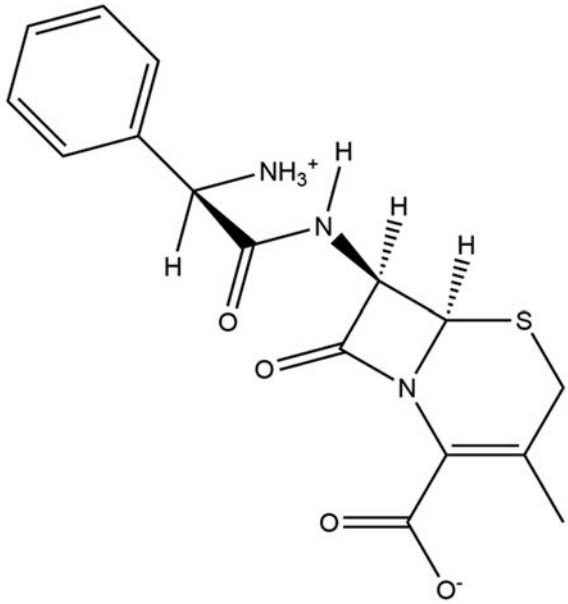

Figure 1. The molecular structure of cephalexin.

[a]Author to whom correspondence should be addressed. Electronic mail: kaduk@polycrystallography.com

 0885-7156/2020/35(4)/293/8/$18.00

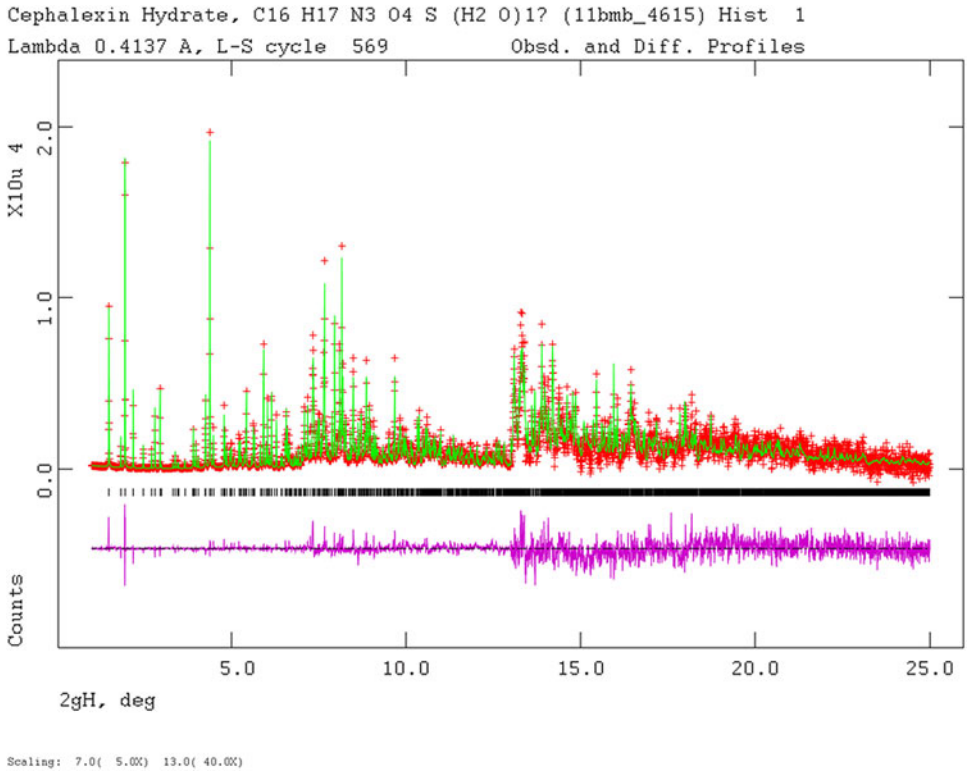

Figure 2. (Color online) The Rietveld plot for the refinement of cephalexin monohydrate. The red crosses represent the observed data points, and the magenta line is the difference (observed – calculated) pattern. The vertical scale has been multiplied by a factor of 5× for $2\theta > 7.0°$, and by a factor of 40× for $2\theta > 13.0°$.

II. EXPERIMENTAL

Cephalexin monohydrate was a commercial reagent, purchased from United States Pharmacopeial Convention (Lot #K0J198), and was used as-received. The white powder was packed into a 1.5 mm diameter Kapton capillary and rotated during the measurement at ~50 Hz. The powder pattern was measured at 295 K at beam line 11-BM (Lee *et al.*, 2008; Wang *et al.*, 2008) of the Advanced Photon Source at Argonne National Laboratory using a wavelength of 0.413693 Å from 0.5° to 50° 2θ with a step size of 0.001° and a counting time of 0.1 s/step.

The pattern was indexed on a monoclinic unit cell with $a = 16.7522$, $b = 11.9187$, $c = 27.0468$ Å, $\beta = 107.031°$, $V = 5163.45$ Å^3, and $Z = 12$ using DICVOL06 (Louër and Boultif, 2007). Analysis of the systematic absences using EXPO2013 (Altomare *et al.*, 2013) suggested the space group $I2$. Indexing the pattern using Jade 9.5 (MDI, 2014) yielded the equivalent C-centered cell, which was used for

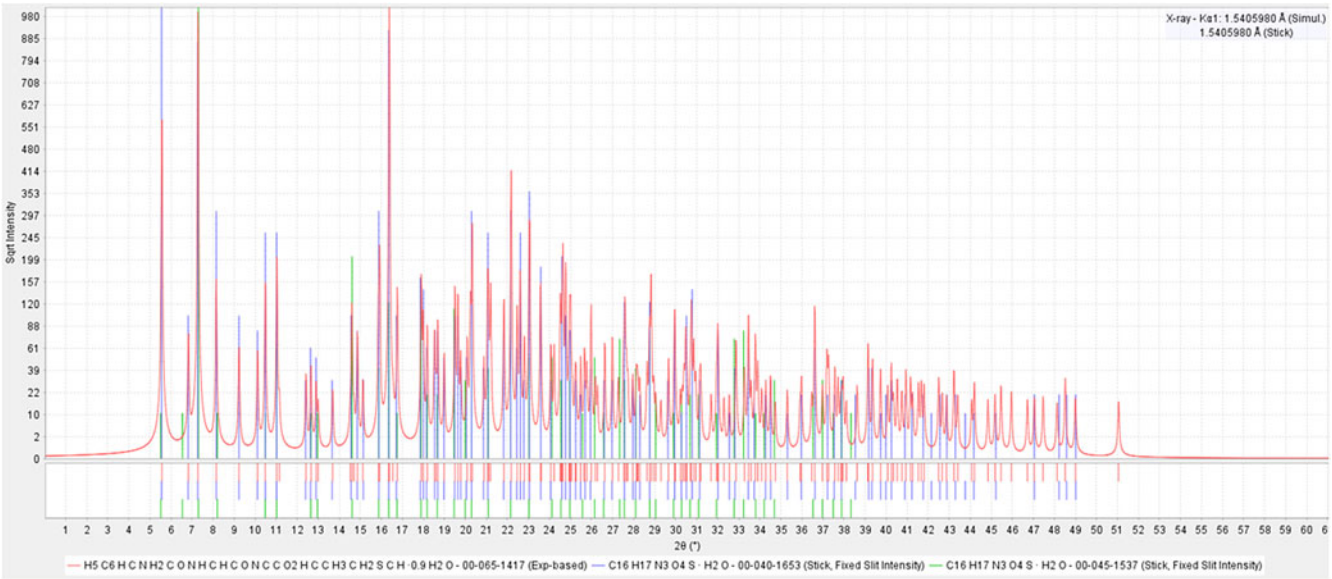

Figure 3. (Color online) Comparison of this pattern of cephalexin monohydrate (red) (PDF entry 00-065-1417, converted to Cu$K\alpha$ wavelength) to the other patterns of this compound reported in PDF entries 00-040-1653 (blue sticks) and 00-045-1537 (green sticks).

https://doi.org/10.1017/S0885715620000627 Published online by Cambridge University Press

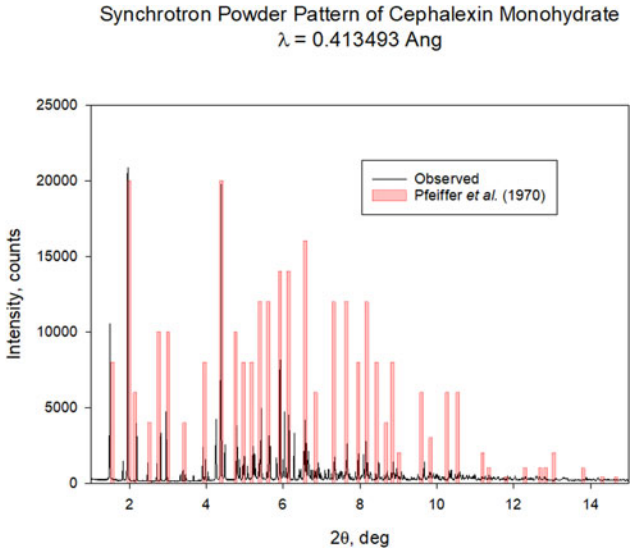

Figure 4. (Color online) Comparison of this synchrotron pattern of cephalexin monohydrate to that reported by Pfeiffer *et al.* (1970) converted to the synchrotron wavelength of 0.413693 Å.

the structure solution and refinement, as the β angle was closer to 90°.

A reduced cell search in the Cambridge Structural Database (Groom *et al.*, 2016) yielded three hits but no cephalexin structures. A name search on "cephalexin" yielded the structure of cephalexin dihydrate (Kennedy *et al.*, 2003; Refcode BEBNIG), as well as the structure of a *bis*(cephalexin) β-naphthol 5.5 hydrate (Kemperman *et al.*, 1999; Refcode GUCSEC).

After several attempts to solve the structure using Monte Carlo-simulated annealing techniques with multiple programs failed to yield plausible results, a different strategy was used. We noted that the lattice parameters were not very different from those of BEBNIG. The BEBNIG lattice parameters were changed to those of the current *C*-centered monoclinic cell, the (disordered) water molecules were removed, and the structure was optimized using the Forcite module of Materials Studio (Dassault Systèmes, 2014). A successful refinement was begun from this model. It might be said that the structure was solved by "isomorphous replacement".

Rietveld refinement was carried out using GSAS (Toby, 2001; Larson and Von Dreele, 2004). Only the 1.0°–25.0° portion of the pattern was included in the refinement (d_{min} = 0.955 Å); no significant peaks were observed at higher angles. The three C_6H_5 phenyl rings were refined as rigid bodies. All other non-H-bond distances and angles were subjected to restraints based on a Mercury/Mogul Geometry Check (Bruno *et al.*, 2004; Sykes *et al.*, 2011) of the molecule. The Mogul average and standard deviation for each quantity were used as the restraint parameters. The restraints contributed 5.6% to the final χ^2. The initial refinement did not include the three water molecules. The locations of the oxygen atom were established by successive difference Fourier maps. The initial positions of the active hydrogen atoms were derived based on potential hydrogen bonding patterns. The U_{iso} were grouped by chemical similarity, and the U_{iso} in the three independent cephalexin molecules were constrained to be identical. The hydrogen atoms were included in calculated positions, which were recalculated during the refinement. The U_{iso} of the hydrogen atoms were constrained to be 1.3× that of the heavy atom to which they are attached. The peak profiles were described using profile function #4 (Thompson *et al.*, 1987; Finger *et al.*, 1994), which includes the Stephens (1999) anisotropic strain broadening model. The background was modeled using a three-term shifted Chebyshev polynomial, with a seven-term diffuse scattering function to model the Kapton capillary and any amorphous component. The refinement of 225 variables using 24003 observations and 252 restraints yielded the residuals R_{wp} = 0.0879, R_p = 0.0707, and χ^2 = 2.772. The largest peak (2.33 Å from N13c) and hole (1.86 Å from C29c) in the difference Fourier map were 0.45 and −0.33 eÅ^{-3}, respectively. The Rietveld plot is included as Figure 2. The largest errors are

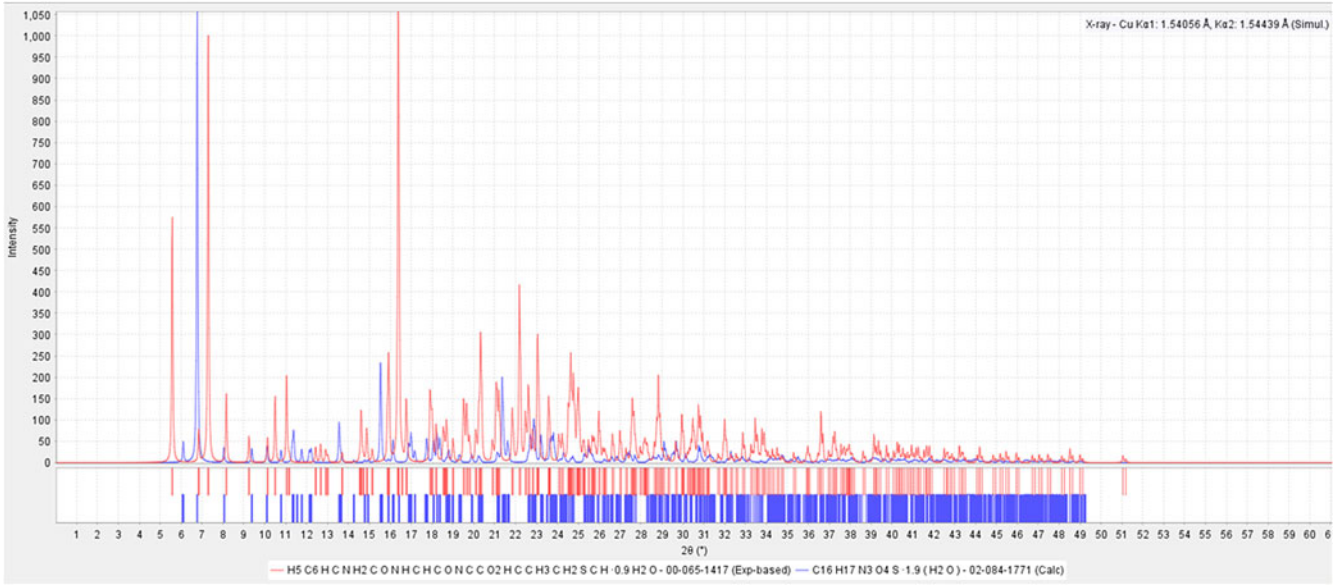

Figure 5. (Color online) Comparison of this pattern of cephalexin monohydrate (red) (PDF entry 00-065-1417, converted to Cu$K\alpha$ wavelength) to the pattern of cephalexin dihydrate (blue) from PDF entry 02-084-1771 (Kennedy *et al.*, 2003).

https://doi.org/10.1017/S0885715620000627 Published online by Cambridge University Press

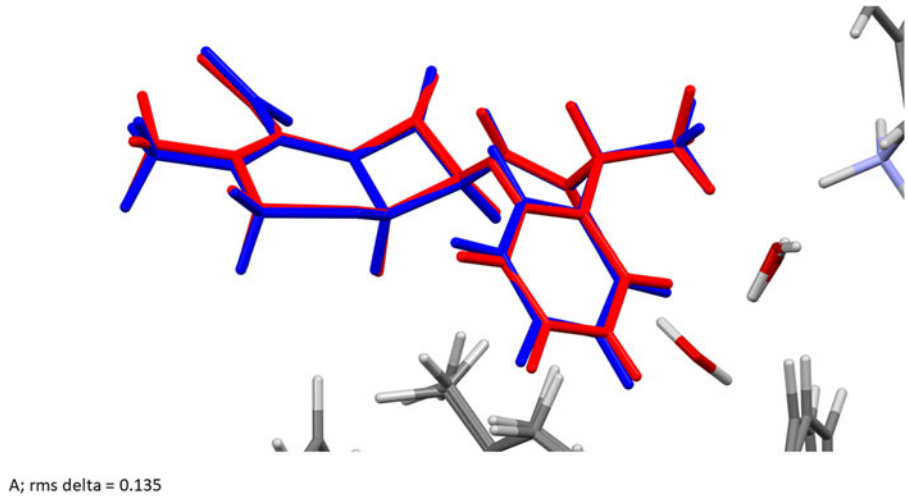

Figure 6. (Color online) Comparison of the Rietveld-refined (red) and VASP-optimized (blue) structures of molecule *a* of cephalexin monohydrate. The rms Cartesian displacement is 0.135 Å.

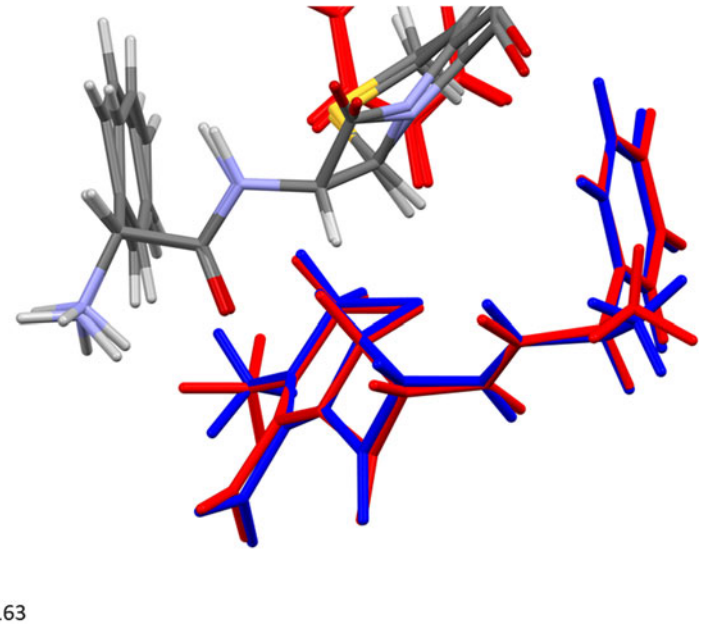

Figure 7. (Color online) Comparison of the Rietveld-refined (red) and VASP-optimized (blue) structures of molecule *b* of cephalexin monohydrate. The rms Cartesian displacement is 0.163 Å.

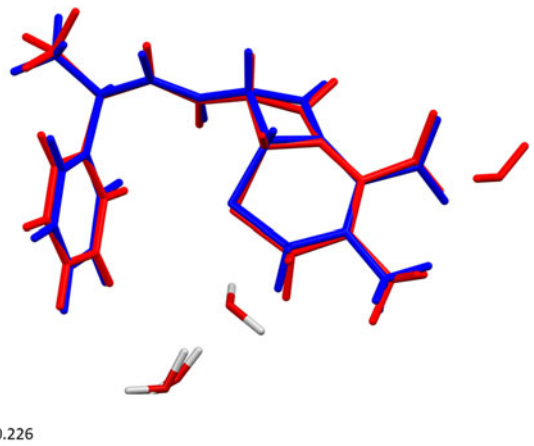

Figure 8. (Color online) Comparison of the Rietveld-refined (red) and VASP-optimized (blue) structures of molecule *c* of cephalexin monohydrate. The rms Cartesian displacement is 0.226 Å.

in the shapes and positions of some of the low-angle peaks and may indicate subtle changes in the sample during the measurement.

A density functional geometry optimization (fixed experimental unit cell) was carried out using VASP (Kresse and Furthmüller, 1996) through the MedeA graphical interface (Materials Design, 2016). The calculation was carried out on 16 2.4 GHz processors (each with 4 Gb RAM) of a 64-processor HP Proliant DL580 Generation 7 Linux cluster at North Central College. The calculation used the GGA-PBE functional, a plane wave cutoff energy of 400.0 eV, and a *k*-point spacing of 0.5 $Å^{-1}$ leading to a $3 \times 3 \times 1$ mesh, and took ~8.4 days. A single-point calculation on the VASP-optimized structure was carried out using CRYSTAL14 (Dovesi *et al.*, 2014). The basis sets for the H, C, N, and O atoms were those of Gatti *et al.* (1994), and the basis set for S was that of Peintinger *et al.* (2013). The calculation was run on eight 2.1 GHz Xeon cores (each with 6 Gb

https://doi.org/10.1017/S0885715620000627 Published online by Cambridge University Press

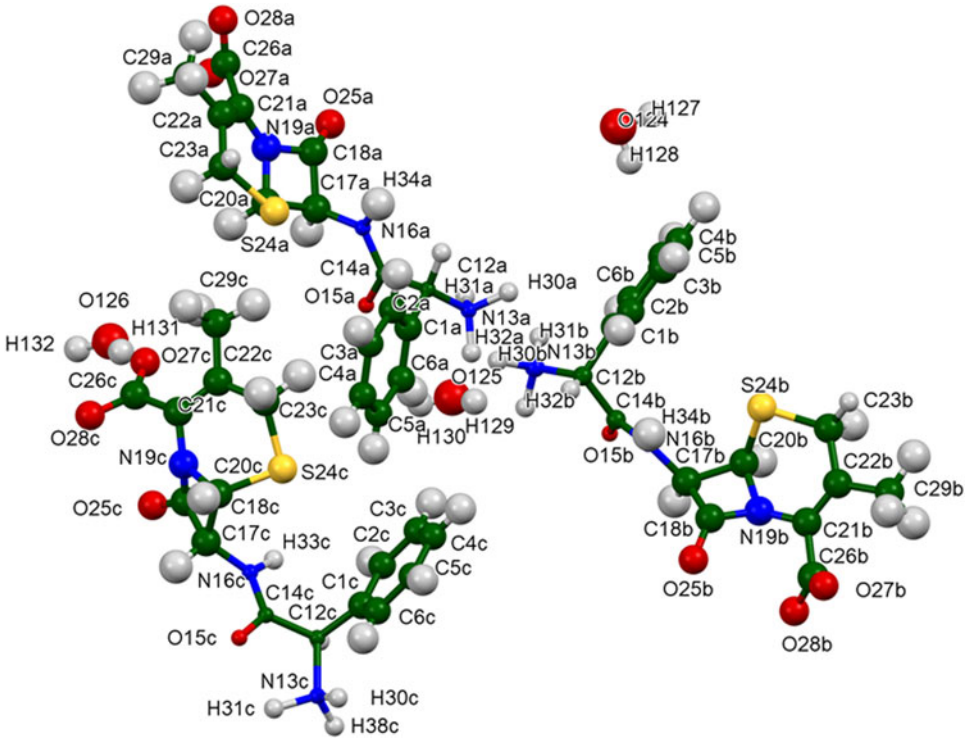

Figure 9. (Color online) The asymmetric unit of cephalexin monohydrate, with the atom numbering. The atoms are represented by 50% probability spheroids.

RAM) of a 304-core Dell Linux cluster at IIT, using 8 *k*-points and the B3LYP functional, and took ~37 h.

III. RESULTS AND DISCUSSION

The synchrotron powder pattern of this study matches those of PDF entries 00-040-1653 and 00-045-1537 (Figure 3) and that of Pfeiffer *et al.* (1970) well enough (Figure 4) to conclude that all four samples contain the same crystalline phase, and thus that this pattern is representative of material in commerce. The powder pattern of cephalexin monohydrate is very different from that of the reported dihydrate (Figure 5).

The refined atom coordinates of cephalexin monohydrate and the coordinates from the DFT optimization have been deposited with ICDD. The root-mean-square Cartesian displacement of the non-hydrogen atoms in the Rietveld-refined and DFT-optimized structures of the three independent cephalexin molecules are 0.135, 0.163, and 0.226 Å (Figures 6–8). The good agreement provides evidence that the experimental structure is correct (van de Streek and Neumann, 2014). This discussion concentrates on the DFT-optimized structure. The asymmetric unit (with atom numbering) is illustrated in Figure 9, and the crystal structure is presented in Figure 10.

The crystal structure is characterized by alternating layers of hydrogen bonds and van der Waals contacts parallel to the

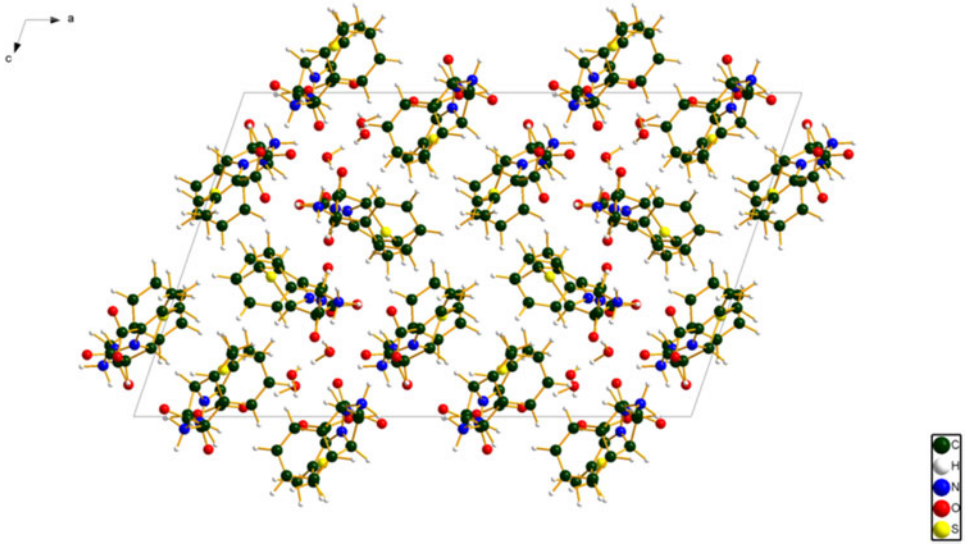

Figure 10. (Color online) The crystal structure of cephalexin monohydrate viewed down the *b*-axis.

https://doi.org/10.1017/S0885715620000627 Published online by Cambridge University Press

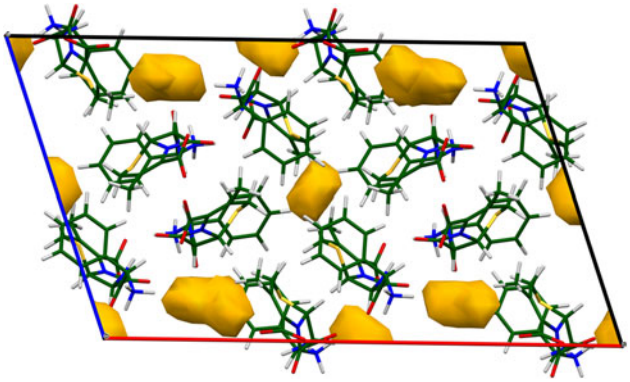

Figure 11. (Color online) Voids in the structure of cephalexin monohydrate after the water molecules are removed. The probe radius was 1.0 Å.

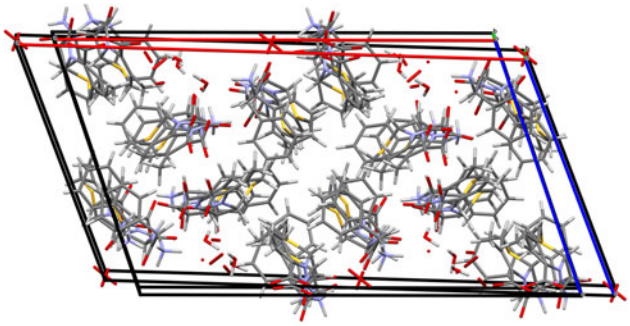

Figure 12. (Color online) Comparison of the crystal structures of cephalexin monohydrate and cephalexin dihydrate. The Mercury Structure Overlay tool was used to fit the positions of all 12 sulfur atoms in the unit cell.

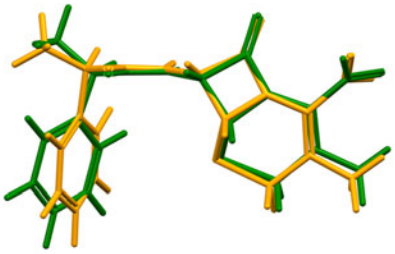

Figure 13. (Color online) Comparison of cephalexin molecule *a* (green) and molecule *b* (orange). The rms Cartesian displacement is 0.434 Å.

bc-plane. The water molecules occur in clusters (Figure 11), occupying one of the apparent voids (probe radius in Mercury decreased to 1.0 Å). The general arrangement of the cephalexin molecules is similar in the monohydrate and dihydrate structures (Figure 12), but the differences in the lattice parameters and structural details cause the powder patterns to be very different.

All of the bond distances, angles, and torsion angles fall within the normal ranges indicated by a Mercury Mogul Geometry check (Macrae *et al.*, 2020). The three independent cephalexin molecules exhibit different conformations (Figures 13–15) with root-mean-square Cartesian displacements of *a*/*b* = 0.434, *a*/*c* = 0.719, and *b*/*c* = 0.332 Å, respectively.

Figure 14. (Color online) Comparison of cephalexin molecule *b* (orange) and molecule *c* (purple). The rms Cartesian displacement is 0.719 Å.

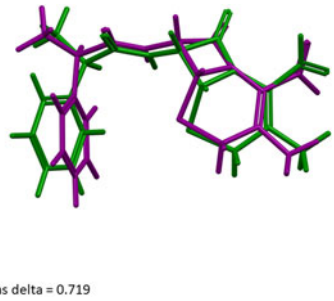

Figure 15. (Color online) Comparison of cephalexin molecule *a* (green) and molecule *c* (purple). The rms Cartesian displacement is 0.332 Å.

Quantum chemical geometry optimization of the cephalexin molecules (DFT/B3LYP/6-31G*/water) using Spartan '18 (Wavefunction, Inc., 2018) indicated that molecules *a* and *b* are within 0.1 kcal mol^{-1} of each other in energy, and that molecule *c* is 76.6 kcal mol^{-1} higher in energy. A molecular mechanics conformational analysis indicated that the minimum-energy conformation is much more compact than the observed ones, with the ammonium and carboxylate groups folded toward each other. Intermolecular interactions are thus important in determining the observed conformations.

Analysis of the contributions to the total crystal energy using the Forcite module of Materials Studio (Dassault, 2014) suggests that angle distortion terms dominate the intramolecular deformation energy, as might be expected in a fused-ring system. The intermolecular energy is dominated by electrostatic repulsions, which in this force-field-based analysis include cation coordination and hydrogen bonds. The hydrogen bonds are better analyzed using the results of the DFT calculation.

Hydrogen bonds are important in the crystal structure (Table I). Five of the six protons in the water molecules act as donors in O–H···O hydrogen bonds. The energies of these hydrogen bonds were calculated using the correlation of Rammohan and Kaduk (2018). The hydrogen atom H128 acts as a donor to two different phenyl ring carbon atoms, to form bifurcated O–H···C hydrogen bonds. Each cephalexin molecule is a zwitterion, containing an ammonium group (N13a, b, and c) and carboxylate groups (C26, O27, O28). As expected, the ammonium ions form N–H···O hydrogen

https://doi.org/10.1017/S0885715620000627 Published online by Cambridge University Press

TABLE I. Hydrogen bonds (CRYSTAL14) in cephalexin monohydrate.

H-bond	D–H (Å)	H···A (Å)	D···A (Å)	D–H···A (Å)	Overlap, *e*	E (kcal mol^{-1})
O126–H132···O15a	0.981	1.942	2.848	152.4	0.027	9.0
O126–H131···O27c	0.998	1.740	2.686	156.7	0.052	12.5
O125–H130···O126	1.012	1.612	2.599	163.5	0.046	11.7
O125–H129···O27a	0.989	1.760	2.621	143.4	0.042	11.2
O124–H128···C3c	0.975	2.560	3.402	144.6	0.022	
O124–H128···C4c	0.975	2.782	3.536	134.6	0.013	
O124–H127···O27c	0.995	1.778	2.773	177.1	0.038	10.7
N13c–H38c···O28b	1.045	1.990	2.946	150.7	0.029	3.9
N13c–H31c···O15c	1.042	2.010*	2.627	115.1	0.040	4.6
N13c–H30c···O28c	1.083	1.652	2.724	169.5	0.072	6.2
N13b–H32b···O15b	1.036	2.082*	2.681	114.4	0.033	4.2
N13b–H31b···O28b	1.067	1.716	2.768	167.7	0.051	5.2
N13b–H30b···O125	1.060	1.714	2.695	151.8	0.042	4.7
N13a–H32a···O125	1.059	1.722	2.762	166.4	0.037	4.4
N13a–H31a···O27b	1.060	1.693	2.750	174.1	0.056	5.5
N13a–H30a···O28a	1.060	1.802	2.844	166.6	0.045	4.9
N16c–H33c···O124	1.044	1.754	2.786	169.0	0.025	3.6
N16b–H34b···O25a	1.032	1.864	2.876	165.7	0.029	3.9
N16a–H34a···O28a	1.039	1.892	2.929	175.0	0.036	4.4
C29c–H41c···C5c	1.096	2.882	3.928	159.6	0.011	
C29c–H39c···S24a	1.103	2.976	3.863	137.6	0.022	
C29b–H40b···C4b	1.093	2.719	3.500	128.1	0.013	
C29b–H40b···C5b	1.093	2.803	3.575	127.5	0.010	
C23c–H37c···C6a	1.100	2.773	3.650	136.3	0.010	
C12b–H33b···O27a	1.101	2.204	3.287	167.6	0.016	
C12a–H33a···C21a	1.098	2.591	3.671	167.3	0.022	
C5a–H10a···S24c	1.091	3.000	3.640	117.9	0.012	
C3a–H8a···S24b	1.090	2.996	3.838	134.4	0.015	

bonds to carboxylate groups and water molecules, as well as to the carbonyl groups O15. The energies of these N–H···O hydrogen bonds were calculated using the correlation of Wheatley and Kaduk (2019). Methyl, methylene, and methyne groups participate in a variety of weak interactions involving phenyl ring carbon atoms, sulfur atoms, and carboxylate groups, forming C–H···C, C–H···S, and C–H···O hydrogen bonds. Two phenyl ring hydrogen atoms also act as donors in C–H···S hydrogen bonds.

The volume enclosed by the Hirshfeld surface (Figure 16; Hirshfeld, 1977; Turner, *et al*., 2017) is 1278.47 Å^3, 98.97% of 1/4 the unit cell volume. The packing density is thus fairly typical. All of the significant close contacts (red in Figure 16) involve the hydrogen bonds. The volume/non-hydrogen atom is 17.2 Å^3.

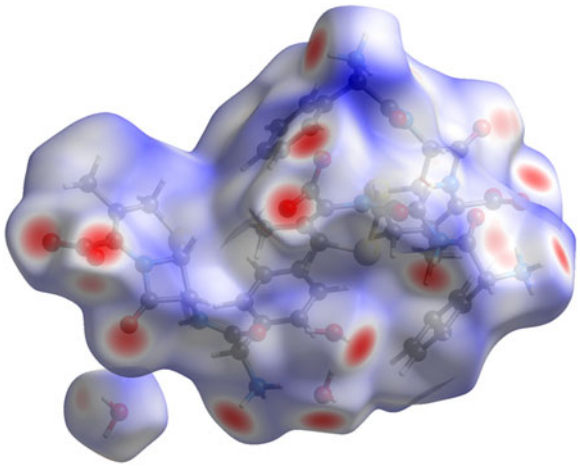

Figure 16. (Color online) The Hirshfeld surface of cephalexin monohydrate. Intermolecular contacts longer than the sums of the van der Waals radii are colored blue, and contacts shorter than the sums of the radii are colored red. Contacts equal to the sums of radii are white.

The Bravais–Friedel–Donnay–Harker (Bravais, 1866; Friedel, 1907; Donnay and Harker, 1937) morphology suggests that we might expect blocky morphology for cephalexin monohydrate, with {001} as the principal faces. A fourth-order spherical harmonic model for preferred orientation was incorporated into the refinement. The texture index was only 1.027, indicating that the preferred orientation was slight in this rotated capillary specimen. The powder pattern of cephalexin monohydrate from this synchrotron data set is included in the Powder Diffraction File as entry 00-065-1417.

IV. DEPOSITED DATA

The Crystallographic Information Framework (CIF) files containing the results of the Rietveld refinement (including the raw data) and the DFT geometry optimization were deposited with the ICDD. The data can be requested at info@icdd.com.

ACKNOWLEDGEMENTS

Use of the Advanced Photon Source at Argonne National Laboratory was supported by the U. S. Department of Energy, Office of Science, Office of Basic Energy Sciences, under Contract No. DE-AC02-06CH11357. This work was partially supported by the International Centre for Diffraction Data. We thank Lynn Ribaud and Saul Lapidus for their assistance in the data collection, and Andrey Rogachev for the use of computing resources at IIT.

https://doi.org/10.1017/S0885715620000627 Published online by Cambridge University Press

CONFLICTS OF INTEREST

The authors have no conflicts of interest to declare.

Altomare, A., Cuocci, C., Giacovazzo, C., Moliterni, A., Rizzi, R., Corriero, N., and Falcicchio, A. (**2013**). "EXPO2013: a kit of tools for phasing crystal structures from powder data," J. Appl. Crystallogr. **46**, 1231–1235.

Bruno, I. J., Cole, J. C., Kessler, M., Luo, J., Motherwell, W. D. S., Purkis, L. H., Smith, B. R., Taylor, R., Cooper, R. I., Harris, S. E., and Orpen, A. G. (**2004**). "Retrieval of crystallographically-derived molecular geometry information," J. Chem. Inf. Sci. **44**, 2133–2144.

Dassault Systèmes (**2014**). *Materials Studio 8.0* (BIOVIA, San Diego, CA).

Donnay, J. D. H. and Harker, D. (**1937**). "A new law of crystal morphology extending the law of Bravais," Am. Mineral. **22**, 446–447.

Dovesi, R., Orlando, R., Erba, A., Zicovich-Wilson, C. M., Civalleri, B., Casassa, S., Maschio, L., Ferrabone, M., De La Pierre, M., D-Arco, P., Noël, Y., Causà, M., and Kirtman, B. (**2014**). "CRYSTAL14: a program for the ab initio investigation of crystalline solids," Int. J. Quantum Chem. **114**, 1287–1317.

Finger, L. W., Cox, D. E., and Jephcoat, A. P. (**1994**). "A correction for powder diffraction peak asymmetry due to axial divergence," J. Appl. Crystallogr. **27**(6), 892–900.

Friedel, G. (**1907**). "Etudes sur la loi de Bravais," Bull. Soc. Fr. Mineral. **30**, 326–455.

Gates-Rector, S. and Blanton, T. (**2019**). "The powder diffraction file: a quality materials characterization database," Powd. Diffr. **39**(4), 352–360.

Gatti, C., Saunders, V. R., and Roetti, C. (**1994**). "Crystal-field effects on the topological properties of the electron-density in molecular crystals - the case of urea," J. Chem. Phys **101**, 10686–10696.

Groom, C. R., Bruno, I. J., Lightfoot, M. P., and Ward, S. C. (**2016**). "The Cambridge structural database," Acta Crystallogr. Sect. B: Struct. Sci., Cryst. Eng. Mater. **72**, 171–179.

Hirshfeld, F. L. (**1977**). "Bonded-atom fragments for describing molecular charge densities," Theor. Chem. Acta **44**, 129–138.

Jenkins, R. and Stevenson, G. (**1990**). "Cephalexin hydrate," ICDD Private Communication; PDF entry 00-045-1537.

Kaduk, J. A., Crowder, C. E., Zhong, K., Fawcett, T. G., and Suchomel, M. R. (**2014**). "Crystal structure of atomoxetine hydrochloride (Strattera), $C_{17}H_{22}NOCl$," Powd. Diffr. **29**(3), 269–273.

Kemperman, G. J., de Gelder, R., Dommerholt, F. J., Raemakers-Franken, P. C., Klunder, A. J. H., and Zwanenburg, B. (**1999**). "Clathrate-type complexation of cephalosporins with β-naphthol," Chem. Eur. J. **5**, 2163–2168.

Kennedy, A. R., Okoth, M. O., Sheen, D. B., Sherwood, J. N., Teat, J., and Vrcelj, R. M. (**2003**). "Cephalexin: a channel hydrate," Acta Cryst. C. **59**, o650–o652.

Kresse, G. and Furthmüller, J. (**1996**). "Efficiency of ab-initio total energy calculations for metals and semiconductors using a plane-wave basis set," Comput. Mater. Sci. **6**, 15–50.

Larson, A. C. and Von Dreele, R. B. (**2004**). General Structure Analysis System, (GSAS) (Los Alamos National Laboratory Report LAUR 86-784).

Lee, P. L., Shu, D., Ramanathan, M., Preissner, C., Wang, J., Beno, M. A., Von Dreele, R. B., Ribaud, L., Kurtz, C., Antao, S. M., Jiao, X., and Toby, B. H. (**2008**). "A twelve-analyzer detector system for high-resolution powder diffraction," J. Synch. Rad. **15**(5), 427–432.

Louër, D. and Boultif, A. (**2007**). "Powder pattern indexing and the dichotomy algorithm," Z. Kristallogr. Suppl. **2007**, 191–196.

Macrae, C. F., Sovago, I., Cottrell, S. J., Galek, P. T. A., McCabe, P., Pidcock, E., Platings, M., Shields, G. P., Stevens, J. S., Towler, M., and Wood, P. A. (**2020**). "*Mercury 4.0*; from visualization to design and prediction," J. Appl. Crystallogr. **53**, 226–235.

Materials Design (**2016**). *MedeA 2.20.4* (Materials Design Inc., Angel Fire, NM).

MDI (**2014**). *Jade 9.5* (Materials Data Inc., Livermore, CA).

Peintinger, M. F., Vilela Oliveira, D., and Bredow, T. (**2013**). "Consistent Gaussian basis sets of triple-zeta valence with polarization quality for solid-state calculations," J. Comput. Chem. **34**, 451–459.

Pfeiffer, R. R., Yang, K. S., and Tucker, M. A. (**1970**). "Crystal pseudopolymorphism of cephaloglycin and cephalexin," J. Pharm. Sci. **59**, 1809–1814.

Rammohan, A., and Kaduk, J. A. (**2018**). "Crystal structures of alkali metal (Group 1) citrate salts," Acta Cryst. Sect. B: Cryst. Eng. Mater. **74**, 239–252.

Silvestri, H. H. (**1975**). "Process for the production of cephalexin monohydrate," U. S. Patent 3,862,186.

Sonneveld, E. (**1989**). "Cephalexin hydrate," ICDD Grant-in-Aid; PDF entries 00-040-1652 and 1653.

Stephens, P. W. (**1999**). "Phenomenological model of anisotropic peak broadening in powder diffraction," J. Appl. Crystallogr. **32**, 281–289.

Sykes, R. A., McCabe, P., Allen, F. H., Battle, G. M., Bruno, I. J., and Wood, P. A. (**2011**). "New software for statistical analysis of Cambridge Structural Database data," J. Appl. Crystallogr. **44**, 882–886.

Thompson, P., Cox, D. E., and Hastings, J. B. (**1987**). "Rietveld refinement of Debye-Scherrer synchrotron X-ray data from Al_2O_3," J. Appl. Crystallogr. **20**(2), 79–83.

Toby, B. H. (**2001**). "EXPGUI, a graphical user interface for GSAS," J. Appl. Crystallogr. **34**, 210–213.

Turner, M. J., McKinnon, J. J., Wolff, S. K., Grimwood, D. J., Spackman, P. R., Jayatilaka, D., and Spackman, M. A. (**2017**). *CrystalExplorer17* (University of Western Australia). Available at: http://hirshfeldsurface.net.

van de Streek, J. and Neumann, M. A. (**2014**). "Validation of molecular crystal structures from powder diffraction data with dispersion-corrected density functional theory (DFT-D)," Acta Cryst. Sect. B: Struct. Sci. Cryst. Eng. Mater. **70**(6), 1020–1032.

Wang, J., Toby, B. H., Lee, P. L., Ribaud, L., Antao, S. M., Kurtz, C., Ramanathan, M., Von Dreele, R. B., and Beno, M. A. (**2008**). "A dedicated powder diffraction beamline at the advanced photon source: commissioning and early operational results," Rev. Sci. Inst. **79**, 085105.

Wavefunction, Inc. (**2018**). Spartan '18 Version 1.2.0, Wavefunction Inc., 18401 Von Karman Ave., Suite 370, Irvine, CA 92612.

Wheatley, A. M. and Kaduk, J. A. (**2019**). "Crystal structures of ammonium citrates," Powd. Diffr. **34**, 35–43.

https://doi.org/10.1017/S0885715620000627 Published online by Cambridge University Press